Zonal Model of Aerosol Persistence in ICUs: Utilization of Time and Space-resolved Sensor Network

K Glenn[1], J He [1], R Rochlin [1], S Teng[1], JG Hecker [2], I Novosselov [1, *]

[1] Department of Mechanical Engineering

University of Washington

[2] Department of Anesthesiology and Pain Medicine

University of Washington

* Corresponding Author

Abstract

The COVID-19 pandemic heightened public awareness about airborne particulate matter (PM) due to the spread of infectious diseases via aerosols. The persistence of potentially infectious aerosol in public spaces, particularly medical settings, deserves close investigation; however, approaches for rapidly parameterizing the temporospatial distribution of particles released by an infected individual have not been reported in literature. This paper presents a methodology for mapping the movement of aerosol plumes using a network of low-cost PM sensors in ICUs. Mimicking aerosol generation by a patient, we tracked aerosolized NaCl particles functioning as tracers for potentially infectious aerosols. In positive (closed door) and neutral-pressure (open door) ICUs, an aerosol spike was detected outside the room, with up to 6% or 19% of all PM escaping through the door gaps, respectively. The outside sensors registered no aerosol spike in negative-pressure ICUs. The K-means clustering analysis of temporospatial data suggests three distinct zones: (1) near the aerosol source, (2) room periphery, and (3) immediately outside the room. These zones inform two-phase aerosol plume behavior: dispersion of the original aerosol spike throughout the room, and evacuation phase where "well-mixed" PM decayed uniformly. Decay rates were calculated for 4 ICUs in positive, neutral, and negative mode, with negative modes decaying the fastest. This research demonstrates the methodology for aerosol persistence monitoring in medical settings; however, it is limited by a relatively small data set. Future studies need to evaluate medical settings with high risks of infectious disease, assess risks of airborne disease transmission, and optimize hospital infrastructure.

Significance Statement

Airborne infectious diseases, including COVID-19, are a major concern for patients and hospital staff. Here, we develop a systematic methodology for mapping the temporospatial distribution of aerosols in ICUs using a network of low-cost particulate matter (PM) sensors. Our method of analysis provides a perspective on the exfiltration efficiency of ICUs as well as the benefits of rooms that have a negative-pressure mode. Our methods could be extended to other public spaces with a high risk of infectious disease to optimize infrastructure and assess the risk of airborne disease.

1 Introduction

Since early 2020, exposure to the SARS-CoV-2 virus and its variants has been a major concern for patients and hospital staff. Like influenza virus and other respiratory diseases, SARS-CoV-2 is spread by inhaling aerosols containing viable virions. [1-9]. Hospital environments can be particularly susceptible to the spread of infection, and evidence-driven approaches can aid in combatting the spread of airborne diseases. Surfaces and air samples from an ICU with a ready-to-discharge patient previously diagnosed with Covid-19 showed that while all surface samples tested negative, air samples remained positive, implying that SARS-CoV-2 shed and persisted as aerosol days after a patient tests negative. [10] There have been some efforts to model and measure aerosol movements within hospital environments; [11-14]; however, a systematic approach to characterize the fate of aerosols released in the hospital environment has not been reported. The current practice in controlling the spread of infectious aerosols in ICUs utilizes negative pressure rooms. It has been suggested that aerosols may persist in negative pressure ICUs for 20-30 minutes, and healthcare providers working in the patient room should wear fitted

respirator masks and other personal protective equipment (PPE).[4, 15, 16] Without proper characterization, these recommendations remain speculative and may not apply to all ICUs and other medical settings. A data-driven approach can inform more targeted aerosol mitigation strategies to optimize HVAC systems to monitor and minimize the spread of infectious aerosols in medical facilities.

Recent advancements in low-cost particulate matter (PM) sensors led to their extensive use in various applications, such as air quality (AQ) in indoor environments [17-20] and outdoor [21-25], including large scale deployments [26-29] by academic researchers and citizen scientists. Optical PM sensors rely on elastic light scattering providing size-resolved PM concentrations in the 0.3 – 10.0 μm range. The low-cost sensor measurements may suffer from sensor-to-sensor variability due to a lack of quality control and differences between individual components.[30, 31] The scattering light intensity depends on particle size, morphology, complex index of refraction (CRI), and sensor geometry. [32] CRI sensitivity can be addressed by optimizing the design to measure scattered light at multiple angles simultaneously or by employing dual-wavelength techniques. [33, 34] However, these solutions are complex and involve expensive components that are not suitable for compact, low-cost devices.[17] As low-cost sensors find applications in pollution monitoring, various studies have evaluated the performance of low-cost PM sensors in laboratory and field settings.[30, 35-41] These reports show that low-cost sensors yield usable data when calibrated against research-grade reference instruments.[28, 42, 43]

The sensor networks have the potential to provide high spatial and temporal resolution, identifying pollution sources and hotspots, which in turn can lead to the development of intervention strategies for exposure assessment and intervention strategies for susceptible individuals. [44] Data can be fitted to a regression model when analyzing large data sets from

such networks. Still, for a large number of sensors and sequentially collected data, conventional techniques may not suffice. Problems with larger dimensions require sequential (or recursive) estimation approaches.[45] An essential factor in the data analysis to simplify or condense the data is to aggregate data from sensors providing that the specifics of the data (such as the locations of the sensor nodes) are not left out.[46] All sensor networks must also have time synchronization.[46]

There is no single technique for analyzing distributed sensor network data. However, the K-means clustering algorithm has been used in several wireless sensor networks.[47-49] The k-means algorithm is efficient at distributed sensor clustering (the method used in this paper) allowing every node to inform clustering decisions instead of choosing a 'head' node for each cluster. Clustering algorithms are practical in pattern recognition and statistical analysis. [49]

In summary, numerous studies have demonstrated the need for characterizing aerosol persistence in the ICU and other medical settings. There is a lack of space - and time-resolved data on the persistence of aerosols in clinical environments. The few studies that have been reported utilized cumbersome equipment and were qualitative. This paper, for the first time, provides a methodology of obtaining real-time data on the persistence of aerosols in ICUs using a low-cost sensor network. The data from multiple experiments in four ICU rooms was reduced using the K-means analysis yielding zonal models describing aerosol fate in clinical environments, including aerosol generation, dispersion, and evacuation stages. The zonal models allow us to characterize aerosol persistence in the ICU, evaluating the difference between positive, neutral, and negative pressure rooms in terms of aerosol decay rates, distribution patterns, and aerosol exfiltration from the ICU.

2 Methods

We present a low-cost approach for evaluating the effectiveness of ventilation systems in clinical facilities to minimize aerosol dispersal into shared spaces. Experiments were conducted in four ICUs at the University of Washington Medical Center (UWMC). The data capture the spatial and temporal distribution of aerosols in ICUs and the immediate vicinity. We analyzed and modeled the dispersion and exfiltration of aerosols generated in the ICUs gaining insight into the potential for exposure inside and outside the rooms under real-world conditions.

2.1 Low-cost Particulate Matter Monitor

Time and space-resolved 3D aerosol monitoring require compact devices with accurate particle sizing and fast sampling rate.[50] This study utilized custom PM monitors that incorporate PM sensors, humidity and temperature sensors, Wi-Fi, and cellular chips for data transfer.[51] The data can be transmitted in real-time to the database using a Wi-Fi or cellular connection; the secure digital (SD) card is used for onboard data backup. The data acquisition rate was set to 10 seconds. Each unit incorporates Plantower PMS A003 (Plantower, Beijing Ereach Technology Co., Ltd, China). A sensor's photodiode positioned normal to the excitation beam measures the light scattered by the particles in the optical volume. The scattering light intensity is then converted to a voltage signal to estimate PM number density and mass concentration. The PMS provides particle counts in six size bins in the optical diameter range of 0.3-10 µm range and mass concentration (µg/m^3) for PM1, PM2.5, and PM10. In the analysis, we report total particle concentration, i.e., all particles with an optical diameter (d_p) > 0.3 µm. This size fraction can stay suspended in air due to their low settling velocities and are a suitable surrogate for long-lived aerosols that may contain SARS-CoV-2 or other infectious agents. [52, 53] Here, original equipment manufacturer (OEM) calibration is used, as relative measurements are sufficient to

construct a zonal map of the ICU environment.[42] The schematic and photograph of the monitor are shown in Supplementary Figure 1.

2.2 Low-cost Sensor Network

To capture the spatial distribution, we deployed a sensor network consisting of 15-20 PM monitors in a predetermined grid in each ICU and the common areas outside the rooms, see Figure 1. Each monitor in the network is shown as a sphere. The 2-3 hallway sensors are located near the door gap and another in the hallway about 10-20 feet from the door. At least one sensor was placed is in the antechamber in the negative pressure ICUs (see Figure 1). The location of the sensors in a representative ICU shows part of a "standard" sensor location grid, expandable or contractible according to room size. Aerosol particles were generated at the head of the bed, mimicking aerosol release during the patient's coughing, sneezing, or talking.

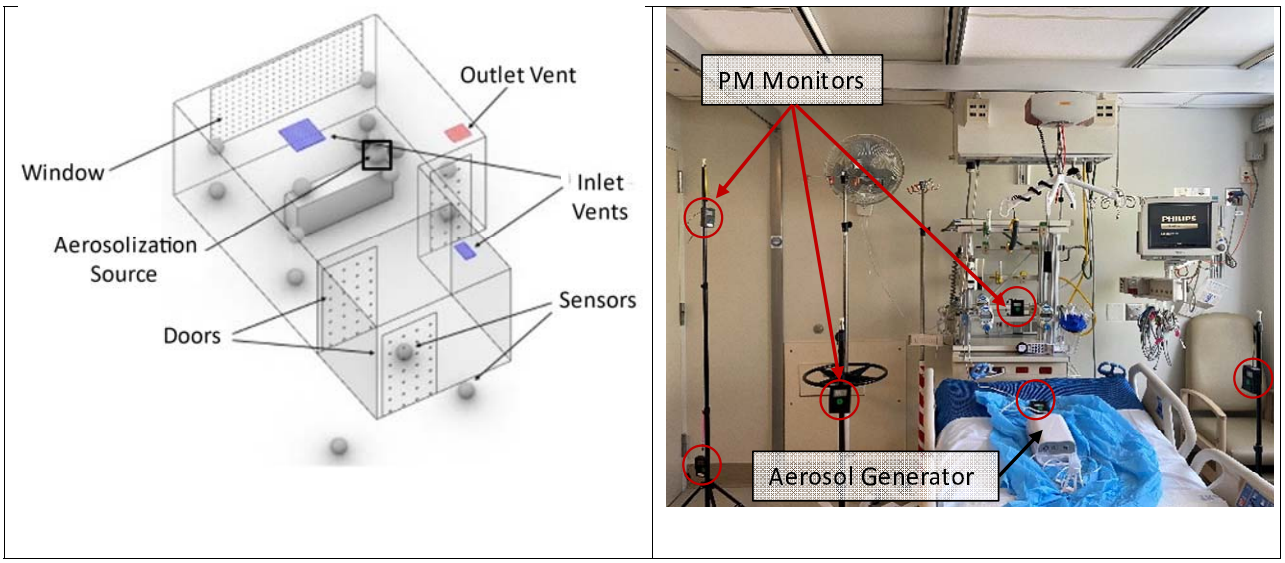

Figure 1: Distributed low-cost sensor network gathers time and space-resolved aerosol information. The data is transmitted to a cloud server, displayed in near real-time, and saved on the SD card internally. Left: Schematic of typical ICU with sensor positions, locations of inlet and outlet vents, windows, and doors. The black square represents the aerosolization source. Right: Photograph of the sensor network set up in ICU.

2.3 Experimental Procedure

In a typical experiment, NaCl particles were generated at the location of the patient's head, and the aerosol concentration was monitored in real-time by the sensor until all PM measurements

returned to the background level. Particles were generated for 60 sec by nebulizing 1% NaCl solution using the MADA Up-Mist™ Medication nebulizer (MADA Products, Carlstadt, NJ, USA), generating particles in 10nm - 2 µm size range.[54] Once aerosolized, particle behavior is governed by aerodynamic properties, and the chemical composition does not affect their persistence in the environment. The 60-second aerosolization was sufficient to produce enough particles for plume tracking but not enough to saturate the sensors and was below detection to trip ICU smoke detectors. The short nebulization produced an initial spike, following which the particle concentration decayed as the air was exchanged via an HVAC system (through air outlets) or escaped through gaps under the doorway or the open door. Experiments were terminated when the aerosol concentration in the room reached the background level, < 1 #/cc (total particle concentration). A short nebulization is also beneficial for getting time-resolved data as a longer nebulization resulted in simultaneous particle generation and evacuation, thereby confounding the analysis.

2.4 Data Collection and Analysis

Particle concentration data with a timestamp from each sensor were recorded every 10 seconds and saved locally to an SD card. Triplicate measurements were made for each condition - doors open (neutral pressure), closed (positive pressure), and negative pressure in ICUs. Based on the spatio-temporal information, the sensors were grouped into zones using K-means clustering. [55] The algorithm iteratively finds a globally optimal partition of the data into a specified number of clusters. [56] A clustering algorithm assigns sensors with similar behavior, such as the 'peak' value and when the peak had occurred during the experiment for each sensor. The K-means optimization was implemented using a custom Python code for each experiment and each ICU.

3 Results and Discussion

3.1 3D Data of Aerosol Distribution

For each experiment, the PM data were first aligned to the start of the nebulization (used as the datum). The sensor readings were averaged in 10-second epochs for each sensor; these data were used to create a time-resolved 3D map of aerosol distribution. The data for each experiment are plotted as a 3D map at given timestamps (Figure 2), as a 2D map (Supplementary Figure 3), and a decay plot as a function of experimental time (Figure 3).

Figure 2 shows a typical 3D resolved aerosol distribution map during the aerosolization and dispersion phases in ICU 1 for positive, neutral, and negative pressure operations. All experiments show the initial concentration spike during aerosolization at the head of the bed and uniform spreading in the dispersion phase. Both positive pressure and neutral pressure conditions showed similar trends. After the initial PM spike during the aerosolization (t=0-60sec), the aerosol concentration in the room reaches a well-mixed state. At ~100 seconds, the particle plume reaches the outer door of the ICU and escapes the room; the particle concentration outside the ICU door reaches its maximum. The particle plume becomes diluted as it enters the common area. The monitor did not register the particles emitted from the room at 10-20 feet away from the ICU door.

The concentration spike near the aerosolization source was the lowest with negative pressure as the aerosol was effectively mixed inside the room. This is likely due to the higher air exchange rate (ACR), resulting in greater air velocities (greater turbulence levels) in the room that enhance mixing. The high ACR resulted in a faster return to the baseline level ~500 seconds than ~800 seconds in the positive and neutral pressure cases. Even more importantly, the outside sensors did not register any spikes in aerosol concentration for negative pressure rooms, indicating that

the particles generated in the ICU remained in the room. This observation confirmed the efficacy of negative pressure ICU for controlling infectious diseases.

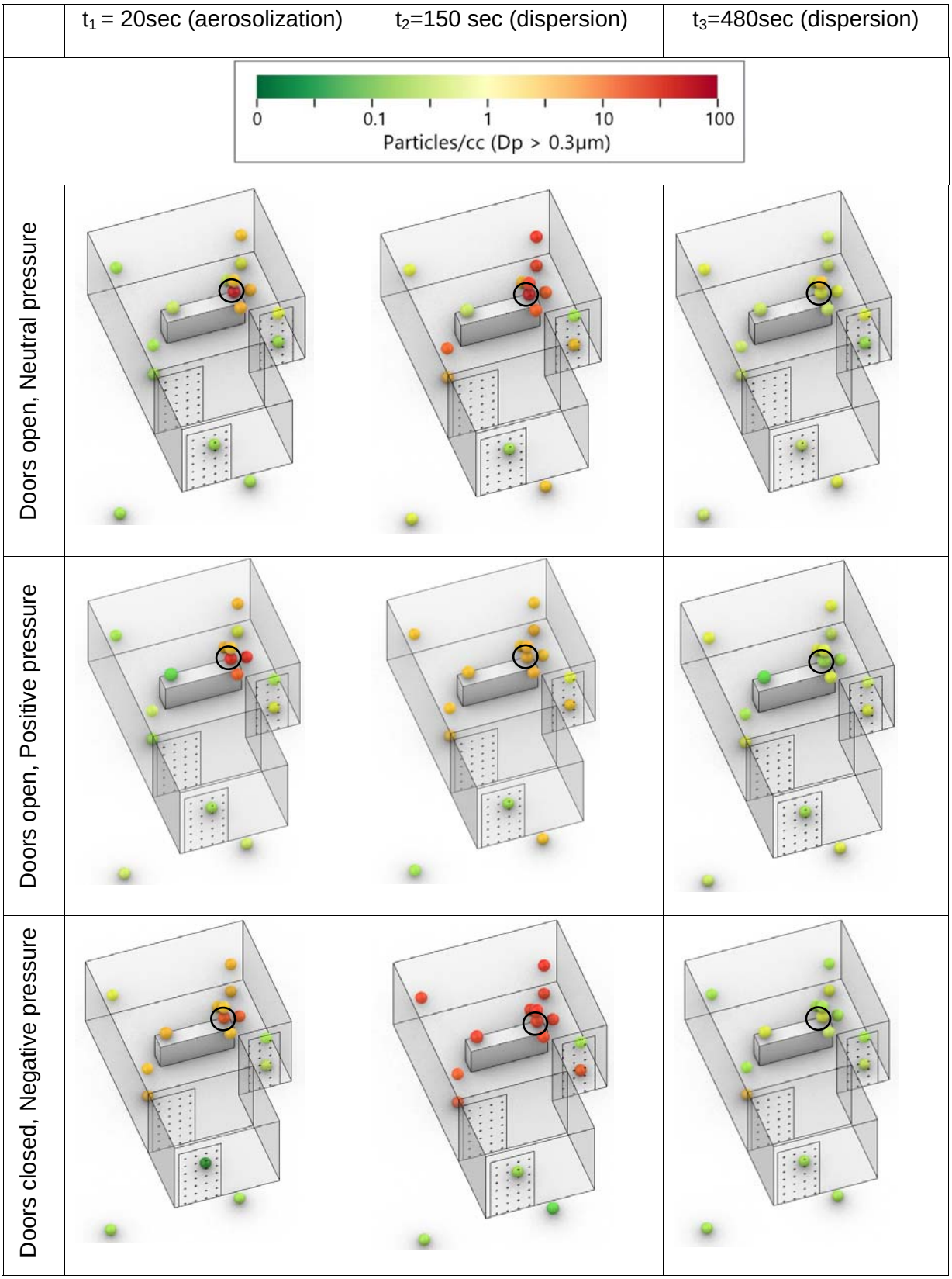

Figure 2: 3D maps from ICU 1 with positive pressure (door closed), neutral pressure (door open), and negative pressure. NaCl particles are nebulized for 60 seconds at the location of the patient's head. Back hallway sensors are located 10-20 feet from the door. The black circle indicates the aerosol source site.

3.2 Zonal Analysis

Based on the spatio-temporal trends, the environment can be split into zones where the aerosol concentrations and persistent trends are similar. While these zones could be assigned based on physical location, the data-driven approach could provide insight into aerosol behavior and persistence without *a priori* assumptions and account for PM sources, sinks, and airflow patterns. The zonal maps based on K-means clustering for ICU 1 are shown in Supplementary Figure 2. Similar to the 3D mapping analysis, the sensor data from three replicate experiments were averaged, and three scenarios (positive, neutral, and negative pressure) were evaluated independently for each ICU. Zone 1 sensors had the largest and the earliest spike in PM concentration. Zone 2 sensors spiked later, and their PM levels were consistent. Zone 3 sensors had a lower and delayed PM spike, or in the negative pressure ICU, did not rise above the background levels. Note that zone assignment is a function of threshold level (variance between the sensors) set by the user, and the zone assignment can vary, depending on these settings. Zone assignment was consistent for each ICU, but the decay rates and the clear-out rates between different ICUs were significantly different, highlighting the robustness of the clustering method and apparent differences between the ICUs. For example, in ICU 1, the algorithm assigned a different sensor split between Zone 1 and Zone 2, and Zone 3 stayed the same; this is likely driven by different room layouts and their ACR. Thus, for further analysis, a zonal map for each ICU was fixed based on the positive pressure ICU data, and each ICU was analyzed separately.

Figure 3 (left) shows the time series of the zonal PM concentrations in ICU 1. Due to variability in initial PM concentration (particles/cc), we normalized the data by dividing all the values by the peak value of that experiment. Consequently, all the decay rates can be plotted on the same scale with the maximum value of unity. For the initial PM loading, the aerosol concentration

returned to the background level (1#cc) in positive and neutral pressure ICU at ~ 800 seconds and negative pressure ICU at ~500 seconds. Individual zone behavior can be generalized as follows:

- Zone 1 -- the concentration spikes immediately with particle generation and then equilibrates to the average room concentration within 30-60 seconds after aerosolization is stopped.
- Zone 2 -- PM concentration begins to rise within 10-30 seconds and reaches the maximum when the initial peak in Zone 1 is reduced but before the aerosol is diluted by the introduction of HVAC filtered air. This indicates that generated aerosol at a point source is first dispersed through the room before it is evacuated by the HVAC system
- Zone 3 -- in the case with positive or neutral pressure, the PM levels are lower than in the room as aerosol plume exits the ICU through the gaps around the door or the open door. The PM levels are at the background level for negative pressure as the air comes into the room from outside.

Though both internal mixing and removal of PM from the room occur simultaneously, the timescale for these processes in the ICU is different by an order of magnitude. The dispersion of the initial spike from Zone 1 to the rest of the room happens over ~30-60 seconds, while the aerosol evacuation (return to the background) takes ~ 500-800 seconds. This separation of time scale suggests that two phases can be identified: (i) dispersion phase and (ii) evacuation phase. The dispersion phase is characterized by the spatial redistribution of the initial PM spike to the room's periphery (from Zone 1 to Zone 2). After the aerosolization is stopped, the PM concentration in Zone 1 rapidly returns to the room's averaged concentration level due to air mixing in the room. During the evacuation phase, the aerosol from a well-mixed room is

removed via an HVAC system or exfiltration through the doors or other openings. The overall air exchange rate and room condition (i.e., door open or closed, the pressure differential between the room and the outside, etc.) governs how fast the room returns to the background PM concentration. In positive and neutral pressure conditions, the aerosol may particle escape from the room (from Zone 2 to Zone 3); in the negative pressure operation, the air from the adjacent environment infiltrates into the ICU following the pressure differential (from Zone 3 to Zone 2). Additional studies are necessary to determine if the distinction between the phases can be generalized to other settings; the indoor settings, ventilation rates, type of aerosol generation sources, filtration strategies, and other variables are likely to play a role in the duration and overlap these phases. The sensor network approach can obtain the necessary temporal and spatial resolution for these analyses.

3.3 Aerosol Decay Rates

The decay rate analysis was performed to generalize the aerosol persistence in the ICUs. During the evacuation phase, the decay rate (DR) was analyzed based on the average of all sensors in the ICU (Zone 1 and Zone 2). The concentration decay appeared linear when plotted on the log-scale against experimental time; however, the decay slopes are different between the ICUs and the operational scenarios. Thus, decay rates were fitted to expression in the form

$$DR=A\ exp\ (bt^{*})),$$

where A is a pre-exponential constant dependent on the PM levels of the initial spike, b is the decay constant, and $t^{*}=(t - t_0)$, or the experimental time (t) minus the time required to reach a well-mixed condition (t_0). In all cases, t_0 was assigned to 120 seconds, or 1 minute after the end of aerosolization. The fits for ICU 1 under positive, neutral, and negative pressure are shown in Figure 3 (right). The decay rates for other ICUs are presented in Table 1.

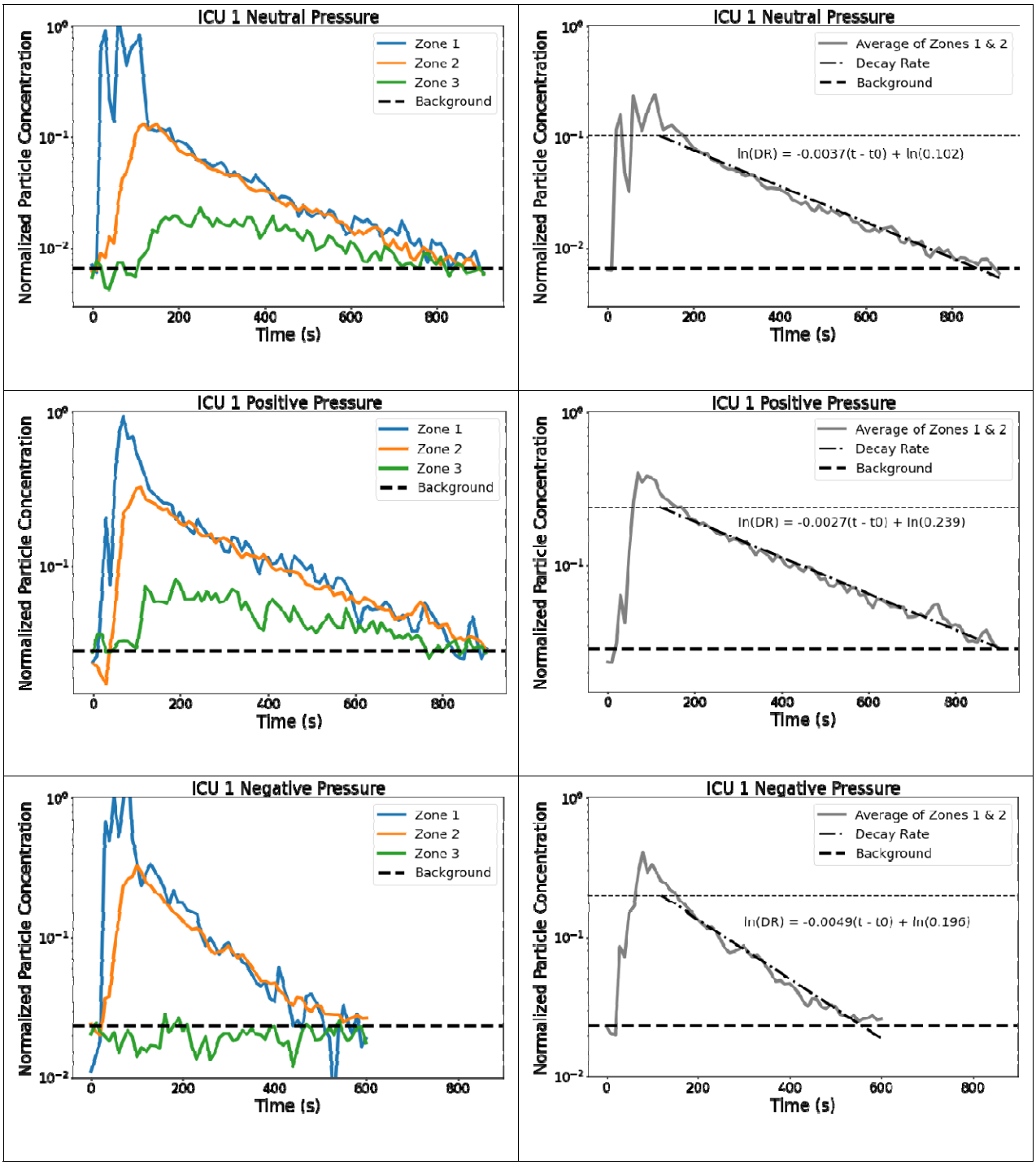

Figure 3: Normalized time data from ICU 1 showing aerosol concentration for each zone. Left: Zones compared to background levels. Right: Normalized average data with decay rate starting 60s after the end of nebulization. The higher horizontal line represents the value of A, or the normalized value of aerosol at which the room becomes well-mixed.

The coefficient (A) is the relative concentration of aerosol when the room reaches well-mixed conditions at t_0. It describes the aerosol dispersion rate for PM generated by a point source. The decay rate exponent (b) characterizes the evacuation process, and it depends on the specific ICU.

For a given ICU, the positive pressure and neutral pressure operation have similar exponents and clear-out times as the experimental procedures and the initial aerosol spike were similar in magnitude between the experiments. The decay rates are calculated from the sensors' data inside the room and do not include the sensors in Zone 3.

The negative pressure operation consistently shows the fastest decay rates for the rooms with negative pressure capabilities, e. g., in ICU1 and ICU3, the negative pressure decay rate is 1.7x greater than neutral and positive pressure rooms. In three ICUs with both neutral and positive pressure measurements, the neutral pressure had a slightly slower decay rate, suggesting that an HVAC system with a closed-door is more efficient at aerosol removal than exfiltration through the open door. However, additional experiments are required to make this conclusion.

Table 1: Decay rate and exfiltration analysis; the first column for each scenario shows the time it takes for the room to return to background levels and the second column show the decay rates.

ICU	Neutral Pressure		Positive Pressure		Negative Pressure	
	Time to Clear (sec)	Decay Rate (DR)	Time to Clear (sec)	Decay Rate (DR)	Time to Clear (sec)	Decay Rate (DR)
ICU 1	821	$0.102\exp(-0.0037t^*)$	830	$0.239\exp(-0.0027t^*)$	450	$0.196\exp(-0.0049t^*)$
ICU 2	502	$0.566\exp(-0.0089t^*)$	565	$0.392\exp(-0.0088t^*)$	N/A	N/A
ICU 3	830	$0.070\exp(-0.0036t^*)$	830	$0.057\exp(-0.0033t^*)$	530	$0.167\exp(-0.0076t^*)$
ICU 4	465	$0.042\exp(-0.0068t^*)$	N/A	N/A	N/A	N/A

Table 2 estimates the fraction of aerosolized microparticles evacuated by the HVAC in the ICU vs. the fraction exfiltrated from the room to the common areas. The analysis was performed for well-mixed conditions by comparing the data from the inside (Zones 1 and 2) and outside the

room (Zone 3). First, the PM concentration recorded by each sensor (#/cc) was corrected to the coverage area (volume) for the particular location, which is possible for the evenly distributed sensor grid and well-mixed PM concentration. Then the particle count from each sensor was added to determine the instantaneous particle count in each zone. In the evacuation phase, the particle count in each zone was integrated in time for the entire experiment, allowing to determine the fraction of aerosolized particles that stayed in the room and were evacuated by HVAC vs. exfiltrated to the shared area. The procedure was performed for each experiment and averaged between three replicates to determine the confidence intervals. The authors recognize that several uncertainties complicate the analysis, such as uneven sensor distribution and non-uniform PM concentration within the Zones; thus, this analysis provides the trends in the aerosol fate assessment and not exact values.

Table 2: Percentage of aerosols that dispersed to each location (inside the room, under the doorway, and at the nursing station) after aerosolization.

ICU	Negative Pressure			Positive Pressure			Neutral Pressure		
	Inside (%)	Doorway (%)	Nurse Station (%)	Inside (%)	Doorway (%)	Nurse Station (%)	Inside (%)	Doorway (%)	Nurse Station (%)
ICU 1	101.8 ± 1.3	-1.2 ± 0.9	-0.5 ± 0.4	97.5 ± 2.7	6.0 ± 0.1	-3.5 ± 2.6	95.1 ± 1.5	5.6 ± 1.8	-0.8 ± 0.5
ICU 2	N/A	N/A	N/A	94.1 ± 1.9	4.3 ± 1.4	1.6 ± 0.6	86.3 ± 4.2	14.2 ± 1.4	0.6 ± 0.3
ICU 3	103.4 ± 0.8	-2.5 ± 0.5	-0.9 ± 0.3	101.3 ± 0.9	-0.3 ± 0.9	-1.0 ± 0.0	97.5 ± 2.0	2.9 ± 1.8	-0.5 ± 0.3
ICU 4	N/A	N/A	N/A	N/A	N/A	N/A	79.8 ± 2.1	18.5 ± 1.3	1.7 ± 1.0

The zone immediately outside of the ICU in the neutral and positive pressure scenarios shows the presence of fugitive aerosols. The open door cases show the highest amount of exfiltrated aerosols from the ICU ~ 2.4% - 20.2%, the close-door positive pressure case ~0% - 5.9%. In the experiments with closed-doors negative pressure, no fugitive aerosols were detected. The nursing stations outside the ICU (10-20 ft away from the ICU) did not show a spike in the PM levels. ICUs 1 and 3 had the option to have a negative pressure configuration and were thus the only

ICUs with antechambers. ICUs 2 and 4 have the highest percentages of aerosol leaving the room, likely due to not having an antechamber.

4 Conclusions

These experiments provide the baseline for evaluating the persistence and fate of aerosols in both ICUs and non-ICU clinical spaces. Negative pressure ICUs consistently evacuated aerosol 1.8x faster than neutral or positive-pressure rooms. The negative pressure rooms effectively eliminated aerosol leaks from ICUs; however, positive and neutral pressure rooms let up to 6% and 19% of aerosols escape, respectively. This suggests that closing the door could prevent up to 13% of aerosol leakage, protecting health care workers and patients outside an ICU. The nursing stations 10-20 feet outside each ICU consistently did not show PM spikes from the aerosol generation in the ICU. Negative pressure ICUs clear aerosols to background levels up to 1.6-1.8x faster than a positive-pressure room. Though negative pressure rooms were clearly superior for managing the amount of aerosol in a room and controlling leakage, the presence of an antechamber also reduced the number of aerosols leaving the room.

The use of the sensor network measurements informed the development of a reduced-order zonal model for aerosol distribution in ICUs under positive, neutral, and negative pressure. Zonal assignment from an unsupervised learning algorithm provided similar results to the zones found by dividing the room into zones spatially, demonstrating that this methodology is generalizable and expandable to other hospital environments (operating rooms, emergency departments, etc.) or non-healthcare areas such as gyms, restaurants, schools, and office buildings. The proposed dispersion and decay rate analysis can be applied to any indoor/outdoor aerosol transport system.

It can be beneficial for exposure risk assessment, optimization of HVAC infrastructure, and the development of intervention strategies.

IRB Approval. After consultation with our IRB, it was determined that no IRB was necessary as we made no measurements involving humans.

References:

1. Foocharoen, C., et al., *Aerosol components associated with hospital mortality in systemic sclerosis: an analysis from a nationwide Thailand healthcare database.* Scientific Reports, 2021. **11**(1).
2. Fabian, P., et al., *Influenza Virus in Human Exhaled Breath: An Observational Study.* PLoS ONE, 2008. **3**(7): p. e2691.
3. Cowling, B.J., et al., *Aerosol transmission is an important mode of influenza A virus spread.* Nature Communications, 2013. **4**(1).
4. Guo, Z.-D., et al., *Aerosol and Surface Distribution of Severe Acute Respiratory Syndrome Coronavirus 2 in Hospital Wards, Wuhan, China, 2020.* Emerging Infectious Diseases, 2020. **26**(7): p. 1583-1591.
5. Pandey, N., et al., *Awareness of aerosol-related transmission of COVID-19 among the dentists of Nepal.* BDJ Open, 2021. **7**(1).
6. Tang, S., et al., *Aerosol transmission of SARS-CoV-2? Evidence, prevention and control.* Environment International, 2020. **144**: p. 106039.

7. Mürbe, D., et al., *Aerosol emission in professional singing of classical music.* Scientific Reports, 2021. **11**(1).

8. Tian, J., et al., *Impacts of primary emissions and secondary aerosol formation on air pollution in an urban area of China during the COVID-19 lockdown.* Environment International, 2021. **150**: p. 106426.

9. Kumar, P., et al., *The nexus between in-car aerosol concentrations, ventilation and the risk of respiratory infection.* Environment International, 2021. **157**: p. 106814.

10. Jin, T., et al., *SARS-CoV-2 presented in the air of an intensive care unit (ICU).* Sustainable Cities and Society, 2021. **65**.

11. Gogate, U. and J.W. Bakal. *Smart Healthcare Monitoring System based on Wireless Sensor Networks*. in *2016 International Conference on Computing, Analytics and Security Trends (CAST)*. 2016. IEEE.

12. Silva, R., et al. *Wireless Sensor Networks in Intensive Care Units*. in *2009 IEEE International Conference on Communications Workshops*. 2009. IEEE.

13. Liu, Y., et al., *Aerodynamic analysis of SARS-CoV-2 in two Wuhan hospitals.* Nature, 2020. **582**(7813): p. 557-560.

14. Crawford, C., et al., *Modeling of aerosol transmission of airborne pathogens in ICU rooms of COVID-19 patients with acute respiratory failure.* Scientific Reports, 2021. **11**(1).

15. Stieglitz, S., *The ICU*, in *Covid-19 Airway Management and Ventilation Strategy for Critically Ill Older Patients*. 2020, Springer International Publishing. p. 183-188.

16. Ong, S.W.X., et al., *Environmental contamination in a coronavirus disease 2019 (COVID-19) intensive care unit—What is the risk?* Infection Control & Hospital Epidemiology, 2021. **42**(6): p. 669-677.

17. Makhsous, S., et al., *Methodology for Addressing Infectious Aerosol Persistence in Real-Time Using Sensor Network.* Sensors, 2021. **21**(11): p. 3928.

18. Hegde, S., et al., *Indoor household particulate matter measurements using a network of low-cost sensors.* Aerosol and Air Quality Research, 2020. **20**(2): p. 381-394.

19. Li, J., et al., *Spatiotemporal distribution of indoor particulate matter concentration with a low-cost sensor network.* Building and Environment, 2018. **127**: p. 138-147.

20. Kumar, P., et al., *Real-time sensors for indoor air monitoring and challenges ahead in deploying them to urban buildings.* Science of the Total Environment, 2016. **560**: p. 150-159.

21. Seto, E., et al. *Use of low-cost particle monitors to calibrate traffic-related air pollutant models in urban areas*. in *International Environmental Modelling and Software Society*. 2014.

22. Liu, X., et al., *Low-cost sensors as an alternative for long-term air quality monitoring.* Environmental research, 2020. **185**: p. 109438.

23. Kuhn, T., et al., *Air quality during and after the Commonwealth Games 2018 in Australia: Multiple benefits of monitoring.* Journal of Aerosol Science, 2021. **152**: p. 105707.

24. Jiao, W., et al., *Community Air Sensor Network (CAIRSENSE) project: evaluation of low-cost sensor performance in a suburban environment in the southeastern United States.* Atmospheric Measurement Techniques, 2016. **9**(11): p. 5281-5292.

25. Gao, M., J. Cao, and E. Seto, *A distributed network of low-cost continuous reading sensors to measure spatiotemporal variations of PM2.5 in Xi'an, China.* Environmental Pollution, 2015. **199**: p. 56-65.

26. Kumar, P., et al., *The rise of low-cost sensing for managing air pollution in cities.* Environment international, 2015. **75**: p. 199-205.

27. Li, J., et al., *Integrating low-cost air quality sensor networks with fixed and satellite monitoring systems to study ground-level PM2. 5.* Atmospheric Environment, 2020. **223**: p. 117293.

28. Chao, C.-Y., et al., *Integrating Fixed Monitoring Systems with Low-Cost Sensors to Create High-Resolution Air Quality Maps for the Northern China Plain Region.* ACS Earth and Space Chemistry, 2021. **5**(11): p. 3022-3035.

29. Qiao, X., et al., *Improving data reliability: A quality control practice for low-cost PM2. 5 sensor network.* Science of The Total Environment, 2021. **779**: p. 146381.

30. Austin, E., et al., *Laboratory Evaluation of the Shinyei PPD42NS Low-Cost Particulate Matter Sensor.* PloS one, 2015. **10**(9): p. e0137789.

31. Sousan, S., et al., *Inter-comparison of low-cost sensors for measuring the mass concentration of occupational aerosols.* Aerosol Science and Technology, 2016. **50**(5): p. 462-473.

32. Njalsson, T. and I. Novosselov, *Design and optimization of a compact low-cost optical particle sizer.* Journal of Aerosol Science, 2018. **119**: p. 1-12.

33. Renard, J.-B., et al., *LOAC: a small aerosol optical counter/sizer for ground-based and balloon measurements of the size distribution and nature of atmospheric particles–Part 2: First results from balloon and unmanned aerial vehicle flights.* Atmospheric Measurement Techniques, 2016. **9**(8): p. 3673-3686.

34. Nagy, A., et al., *Numerical and experimental study of the performance of the dual wavelength optical particle spectrometer (DWOPS).* Journal of aerosol science, 2007. **38**(4): p. 467-478.

35. Cordero, J.M., R. Borge, and A. Narros, *Using statistical methods to carry out in field calibrations of low cost air quality sensors.* Sensors and Actuators B: Chemical, 2018. **267**: p. 245-254.

36. Feenstra, B., et al., *Performance evaluation of twelve low-cost PM2. 5 sensors at an ambient air monitoring site.* Atmospheric Environment, 2019. **216**: p. 116946.

37. Kelly, K., et al., *Ambient and laboratory evaluation of a low-cost particulate matter sensor.* Environmental pollution, 2017. **221**: p. 491-500.

38. Sayahi, T., A. Butterfield, and K. Kelly, *Long-term field evaluation of the Plantower PMS low-cost particulate matter sensors.* Environmental pollution, 2019. **245**: p. 932-940.

39. Tryner, J., et al., *Laboratory evaluation of low-cost PurpleAir PM monitors and in-field correction using co-located portable filter samplers.* Atmospheric Environment, 2020. **220**: p. 117067.

40. Wang, Z., W.W. Delp, and B.C. Singer, *Performance of low-cost indoor air quality monitors for PM2. 5 and PM10 from residential sources.* Building and Environment, 2020. **171**: p. 106654.

41. Zusman, M., et al., *Calibration of low-cost particulate matter sensors: Model development for a multi-city epidemiological study.* Environment International, 2020. **134**: p. 105329.

42. Huang, C.-H., et al., *Assessing the value of complex refractive index and particle density for calibration of low-cost particle matter sensor for size-resolved particle count and PM2. 5 measurements.* Plos one, 2021. **16**(11): p. e0259745.

43. Li, J., et al., *Evaluation of nine low-cost-sensor-based particulate matter monitors.* Aerosol and Air Quality Research, 2020. **20**(2): p. 254-270.

44. Duncan, G.E., et al., *Usability of a personal air pollution monitor: Design-feedback iterative cycle study.* JMIR mHealth and uHealth, 2018. **6**(12): p. e12023.

45. Bontempi, G. and Y. Le Borgne. *An adaptive modular approach to the mining of sensor network data*. in *proceedings of 1st International Workshop on Data Mining in Sensor Networks as part of the SIAM International Conference on Data Mining*. 2005. SIAM Press Newport Beach, CA.

46. Akyildiz, I.F., et al., *A survey on sensor networks.* IEEE Communications Magazine, 2002. **40**(8): p. 102-114.

47. Harb, H., et al. *K-means based clustering approach for data aggregation in periodic sensor networks*. in *2014 IEEE 10th International Conference on Wireless and Mobile Computing, Networking and Communications (WiMob)*. 2014. IEEE.

48. Hua, M., et al., *Continuous K-Means Monitoring with Low Reporting Cost in Sensor Networks.* IEEE Transactions on Knowledge and Data Engineering, 2009. **21**(12): p. 1679-1691.

49. Sasikumar, P. and S. Khara. *K-Means Clustering in Wireless Sensor Networks*. in *2012 Fourth International Conference on Computational Intelligence and Communication Networks*. 2012. IEEE.

50. Crilley, L.R., et al., *Evaluation of a low-cost optical particle counter (Alphasense OPC-N2) for ambient air monitoring.* Atmospheric Measurement Techniques, 2018. **11**(2): p. 709-720.

51. Czitrovszky, A., *Environmental applications of solid-state lasers*, in *Handbook of Solid-State Lasers*. 2013, Elsevier. p. 616-646.

52. Lee, B.U., *Minimum Sizes of Respiratory Particles Carrying SARS-CoV-2 and the Possibility of Aerosol Generation.* International Journal of Environmental Research and Public Health, 2020. **17**(19): p. 6960.

53. Pastuszka, J.S., et al., *Bacterial and fungal aerosol in indoor environment in Upper Silesia, Poland.* Atmospheric Environment, 2000. **34**(22): p. 3833-3842.

54. Vaddi, R.S., Y. Guan, and I. Novosselov, *Behavior of ultrafine particles in electro-hydrodynamic flow induced by corona discharge.* Journal of Aerosol Science, 2020. **148**: p. 105587.

55. Likas, A., N. Vlassis, and J. J. Verbeek, *The global k-means clustering algorithm.* Pattern Recognition, 2003. **36**(2): p. 451-461.

56. Krishna, K. and M. Narasimha Murty, *Genetic K-means algorithm.* IEEE Transactions on Systems, Man and Cybernetics, Part B (Cybernetics), 1999. **29**(3): p. 433-439.